Resonant backward scattering of light by a subwavelength metallic slit with two open sides

S. V. Kukhlevsky,[1] M. Mechler,[2] L. Csapó,[3] K. Janssens,[4] and O. Samek[5]
[1]*Institute of Physics, University of Pécs, Ifjúság u. 6, Pécs 7624, Hungary*
[2]*South-Trans-Danubian Cooperative Research Centre, University of Pécs, Ifjúság u. 6, Pécs 7624, Hungary*
[3]*Institute of Mathematics and Information, University of Pécs, Ifjúság u. 6, Pécs 7624, Hungary*
[4]*Department of Chemistry, University of Antwerp, Universiteitsplein 1, B-2610 Antwerp, Belgium*
[5]*Institute of Spectrochemistry and Applied Spectroscopy, Bunsen-Kirchhoff-Str. 11, D-44139 Dortmund, Germany*
(Received 7 June 2005; revised manuscript received 2 August 2005; published 21 October 2005)

The backward scattering of TM-polarized light by a two-side-open subwavelength slit in a metal film is analyzed. We show that the reflection coefficient versus wavelength possesses a Fabry-Perot-like dependence that is similar to the anomalous behavior of transmission reported in the study [Y. Takakura, Phys. Rev. Lett. **86**, 5601 (2001)]. The open slit totally reflects the light at the near-to-resonance wavelengths. In addition, we show that the interference of incident and resonantly backward-scattered light produces in the near-field diffraction zone a spatially localized wave whose intensity is $10-10^3$ times greater than the incident wave, but one order of magnitude smaller than the intracavity intensity. The amplitude and phase of the resonant wave at the slit entrance and exit are different from that of a Fabry-Perot cavity.

DOI: 10.1103/PhysRevB.72.165421 PACS number(s): 78.66.Bz, 42.25.Fx, 07.79.Fc, 42.79.Ag

I. INTRODUCTION

The most impressive features of light scattering by subwavelength metallic nanostructures are resonant enhancement and localization of the light by excitation of electron waves in the metal (for example, see Refs. 1–40). In the last few years, a great number of studies have been devoted to the nanostructures in metal films, namely a single aperture, a grating of apertures, and an aperture surrounded by grooves. Since the recent paper of Ebbesen and colleagues[4] on the resonantly enhanced transmission of light observed for a two-dimensional (2D) array of subwavelength holes in metal films, the resonant phenomenon is intensively discussed in the literature.[9–38] Such a kind of light scattering is usually called a Wood's anomaly. In the early researches, Hessel and Oliner showed that the resonances come from coupling between nonhomogeneous diffraction orders and eigenmodes of the grating.[5] Neviere and co-workers discovered two other possible origins of the resonances.[6,7] One appears when the surface plasmons of a metallic grating are excited. The other occurs when a metallic grating is covered by a dielectric layer, and corresponds to guided mode resonances in the dielectric film. The role of resonant Wood's anomalies and Fano's profiles[8] in the resonant transmission were explained in Ref. 9.

The phenomena involved in propagation through hole arrays are different from those connected with slit arrays. In a slit waveguide there is always a propagating mode inside the channel, while in a hole waveguide all modes are evanescent for hole diameters smaller than approximately a wavelength. In the case of slit apertures in a thick metal film, the transmission exhibits enhancement due to a pure geometrical reason, the resonant excitation of propagating modes inside the slit waveguide.[10–14] At the resonant wavelengths, the transmitted field increases via the strong coupling of an incident wave with the waveguide modes giving a Fabry-Perot-like behavior.[11,14–16] In the case of films, whose thicknesses are too small to support the intracavity resonance, the extraordinary transmission can be caused by another mechanism, the generation of resonant surface plasmon polaritons and coupling of them into radiation.[4,10,12,17,23] Both physical mechanisms play important roles in the extraordinary transmission through arrays of two-side-open slits (transmission gratings) and the resonant reflection by arrays of one-side-open slits (reflection gratings). A model of trapped (waveguide) modes has been recently used to show that an array of two-side-open slits can operate like a reflection grating totally reflecting TE-polarized light.[18] The surface plasmons and Rayleigh anomalies were involved in an explanation of reflective properties of such a kind of grating.[19]

The studies in Refs. 14–16 and 20 have pointed out that the origin of anomalous scattering of light by a grating of slits (holes) can be better understood by clarifying the transmission and reflection properties of a single subwavelength slit. Along this direction, it was already demonstrated that the intensity of TM-polarized light resonantly transmitted through a single slit can be $10-10^3$ times higher than the incident wave[1–3,16] and that the transmission coefficient versus wavelength possesses a Fabry-Perot-like behavior.[14–16] Unfortunately, the reflection properties of the slit have received no attention in the literature. The very recent study of Ref. 18 only concerned the problem by regarding the total reflection of TE-polarized light by a grating of two-side-open slits to properties of the independent slit emitters.

In this paper, the backward scattering of light by a two-side-open subwavelength slit is analyzed. To compare properties of the light reflection with the extraordinary transmission,[14–16] we consider the scattering of TM-polarized light by a slit in a thick metallic film of perfect conductivity. From the latter metal property it follows that surface plasmons do not exist in the film. Such a metal can be described by the Drude model for which the plasmon frequency tends towards infinity. The traditional approach based on the Neerhoff and Mur solution of Maxwell's equations is used in the computations.[1–3] The paper is organized as follows. The theoretical background, numerical analysis,

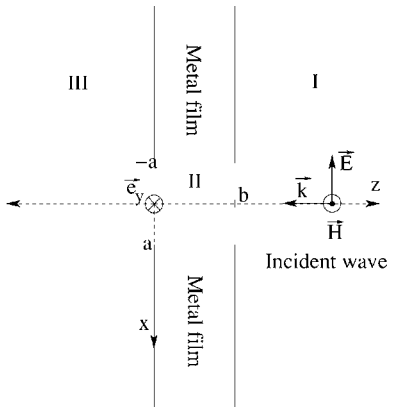

FIG. 1. Propagation of a continuous wave through a subwavelength nanosized slit in a thick metal film.

and discussion are presented in Sec. II. The summary and conclusions are given in Sec. III. The brief description of the model is presented in the Appendix.

II. NUMERICAL ANALYSIS AND DISCUSSION

It is well known that when a light wave is scattered by a subwavelength metallic object, a significant part of the incident light can be scattered backward (reflected) whether the object is reflecting or transparent. It was recently demonstrated that an array of two-side-open subwavelength metallic slits effectively reflects light waves at the appropriate resonant conditions.[18,19] One may suppose that this is true also in the case of a single slit. In this section, we test whether a light wave can be resonantly reflected by a single two-side-open subwavelength metallic slit. To address this question, the energy flux in front of the slit is analyzed numerically for various regimes of the light scattering. In order to compare properties of the light reflection with that of the extraordinary (resonant) transmission,[14–16] we consider the zeroth-order scattering of a time-harmonic wave of TM-polarized light by a slit in a perfectly conducting thick metal film placed in vacuum (Fig. 1).

The energy flux $\vec{S}_I$ in front of the slit is compared with the fluxes $\vec{S}_{II}$ and $\vec{S}_{III}$ inside the slit and behind the slit, respectively. The amplitude and phase of the light wave at the slit entrance and exit are compared with that of a Fabry-Perot cavity. The electric $\vec{E}$ and magnetic $\vec{H}$ fields of the light are computed by using the traditional approach based on the Neerhoff and Mur solution of Maxwell's equations.[1–3] For more details of the model, see the Appendix.

According to the model, the electric $\vec{E}(x,z)$ and magnetic $\vec{H}(x,z)$ fields in front of the slit (region I), inside the slit (region II), and behind the slit (region III) are determined by the scalar fields $U_1(x,z)$, $U_2(x,z)$, and $U_3(x,z)$, respectively. The scalar fields are found by solving the Neerhoff and Mur integral equations. The magnetic field of the incident wave is assumed to be time harmonic and constant in the y direction: $\vec{H}(x,y,z,t)=U(x,z)\exp(-i\omega t)\vec{e}_y$. In front of the slit, the field is decomposed into $U_1(x,z)=U^i(x,z)+U^r(x,z)+U^d(x,z)$. The field $U^i(x,z)$ represents the incident field, which is assumed to be a plane wave of unit amplitude; $U^r(x,z)$ denotes the field that would be reflected if there were no slit in the film; $U^d(x,z)$ describes the backward diffracted field due to the presence of the slit. The time averaged Poynting vector (energy flux) $\vec{S}$ of the electromagnetic field is calculated (in cgs units) as $\vec{S}=(c/16\pi)(\vec{E}\times\vec{H}^*+\vec{E}^*\times\vec{H})$. The reflection coefficient $R=S^{rd}_{int}$ is given by the normalized flux $S^{rd}_n=S^{rd}/S^i$ integrated over the slit width $2a$ at the slit entrance ($z=b$), where S^{rd} is the z component of the backward scattered flux, and S^i is the incident flux along the z direction. The flux $S^{rd}=S^{rd}(U^r,U^d)$ is produced by the interference of the backward scattered fields $U^r(x,z)$ and $U^d(x,z)$. The transmission coefficient $T=S^3_{int}(b)$ is determined by the normalized flux $S^3_n=S^3/S^i$ integrated over the slit width at the slit exit ($z=0$), where the flux z component $S^3=S^3(U^3)$ is produced by the forward scattered (transmitted) field $U^3(x,z)$. Notice that the definitions of the reflection R and transmission T coefficients are equivalent to the more convenient ones defined as the integrated reflected or transmitted flux divided by the integrated incident flux. In the following analysis, the reflection and transmission coefficients are compared to the fluxes S^d_{int} and S^{ird}_{int} obtained by integrating the normalized fluxes $S^d_n=S^d/S^i$ and $S^{ird}_n=S^{ird}/S^i$, respectively.

We analyzed the backward scattering of light for a wide range of scattering conditions determined by values of the wavelength λ, slit width $2a$, and film thickness b. As an example, the reflection coefficient $R=S^{rd}_{int}(b)$ as a function of the film thickness b computed for the wavelength $\lambda=800$ nm and the slit width $2a=25$ nm is shown in Fig. 2(a).

The transmission coefficient $T=S^3_{int}(b)$ and the integrated fluxes $S^d_{int}(b)$ and $S^{ird}_{int}(b)$ are presented in the figure for the comparison. We note the reflection resonances of $\lambda/2$ periodicity with the maxima $R_{max}\approx 2$. In agreement with the previous results,[14–16] one can see also the transmission resonances having the same period, and the peak heights $T\approx 10$ ($T\approx\lambda/2\pi a$) at the resonances. It is worthwhile to note the correlation between the positions of maxima and minima in the reflection and transmission. The resonance positions for the total reflection are somewhat left-shifted with respect to the transmission resonances. The maxima of the transmission coefficient correspond to reflection minima. In Fig. 2(a), one can observe also many satellite peaks in reflection. For one broad minimum, there appears a local reflection maximum, which is characterized by a weak amplitude. The local maxima appear before 400, 800, and 1200 nm. The positions of the local maxima approximately correspond to the S^d_{int} maxima. To clarify a role of the fields U^i, U^r, U^d, and U^3 in the resonant backward scattering, we compared the integrated flux $S^{ird}_{int}(U^i,U^r,U^d)$ with the fluxes $S^d_{int}(U^d)$ and $S^3_{int}(U^3)=T$. One can see from Fig. 2(a) that the flux S^{ird}_{int} produced in front of the slit by the interference of the incident field $U^i(x,z)$ and the backward scattered fields $U^r(x,z)$ and $U^d(x,z)$ is practically undistinguishable from that generated by the backward diffracted field U^d and forward scattered (transmitted) field U^3. The integrated flux $S^{ird}_{int}(a,b)$ as a function of the slit half width a and film thickness b is shown in Fig. 2(b). We notice that the widths and shifts of the reso-

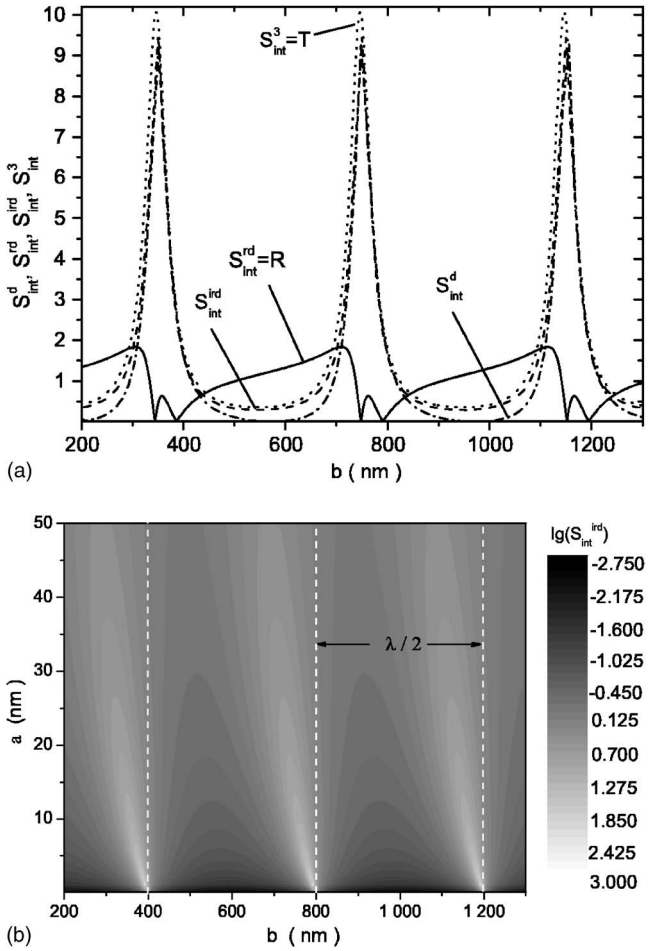

FIG. 2. (a) The reflection coefficient $R=S^{rd}_{int}(b)$, the transmission coefficient $T=S^3_{int}(b)$, and the integrated fluxes $S^d_{int}(b)$ and $S^{ird}_{int}(b)$ as a function of the film thickness b computed for the wavelength $\lambda=800$ nm and the slit width $2a=25$ nm. (b) The logarithm of the integrated flux $S^{ird}_{int}(a,b)$ as a function of the slit half width a and film thickness b.

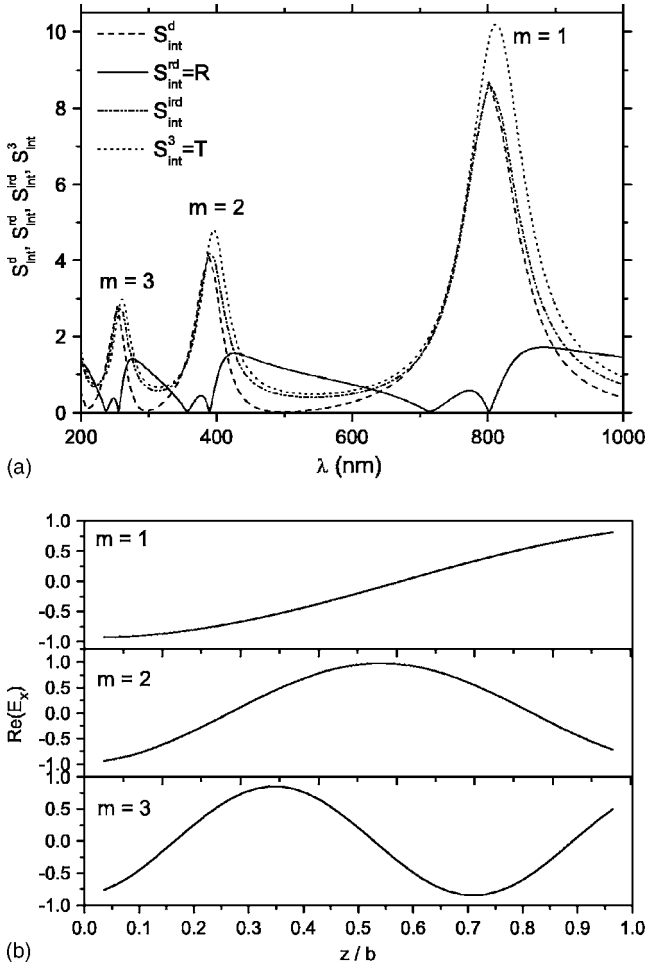

FIG. 3. (a) The reflection coefficient $R=S^{rd}_{int}(\lambda)$, the transmission coefficient $T=S^3_{int}(\lambda)$, and the integrated fluxes $S^d_{int}(\lambda)$ and $S^{ird}_{int}(\lambda)$ versus the wavelength λ computed for the slit width $2a=25$ nm and the screen thickness $b=351$ nm. (b) The real part of the normalized electric field x component $E_x(U_2)=E_x(x,z)$ versus the normalized distance z/b inside the slit cavity at $x=0$, for the resonant wavelength $\lambda^1_r=800$ nm, $\lambda^2_r=389$ nm, and $\lambda^3_r=255$ nm.

nances increase with increasing the value a. Analysis of Fig. 2(a) indicates that the difference between the integrated fluxes $S^{rd}_{int}(U^r,U^d)=R$ and $S^3_{int}(U^3)=T$ $[T\approx S^d_{int}(U^d)]$ appears due to the interference of the backward diffracted field $U^d(x,z)$ and the reflected field $U^r(x,z)$.

The dispersion of the reflection coefficient $R(\lambda)=S^{rd}_{int}(\lambda)$ for the slit width $2a=25$ nm and the screen thickness $b=351$ nm is shown in Fig. 3(a).

The integrated fluxes $S^d_{int}(\lambda)$, $S^{ird}_{int}(\lambda)$, and $S^3_{int}(\lambda)=T(\lambda)$ versus the wavelength are shown in the figure for the comparison. A very interesting behavior of the dispersion is that the coefficient R versus the wavelength λ possesses a Fabry-Perot-like dependence that is similar to the anomalous behavior of transmission $T(\lambda)$ reported in Refs. 11, 14–16, and 20. In agreement with Refs. 1–3 and 16, the height of the first (maximum) transmission peak is given by $T\approx\lambda^1_r/2\pi a$. The wavelengths corresponding to the resonant peaks $\lambda^m_r\approx 2b/m$ $(m=1,2,3,\ldots)$ are in accordance with the results of Ref. 14. The high peak amplitudes (enhancement), however, are different from the low magnitudes (attenuation) predicted in Ref. 14, but compare well with the experimental and theoretical results.[1–3,15,16] The difference is caused by the manner in which the Maxwell equations are solved. Reference 14 uses a simplified approach based on the matching the cavity modes expansion of the light wave inside the slit with the plane waves expansion above and below the slit using two boundary conditions, at $z=0$ and $|z|=b$. Conversely, the Neerhoff and Mur method performs the matching with five boundary conditions, at $z\to 0$, $z\to b$, $x\to a$, $x\to -a$, and $r\to\infty$. In contrast to the sharp Lorentzian-like transmission peaks, the slit forms very wide Fano-type reflection bands [see Fig. 3(a)]. For one broad minimum in reflection, there appears also a local reflection maximum, which is characterized by weak amplitude. At the near-to-resonance wavelengths of the transmission, the open aperture totally reflects the light. It is worthwhile to note the correlation between the wavelengths for maxima and minima in the reflection $R(\lambda)$, transmission $T(\lambda)$, and the flux S^d_{int} (Table I).

The resonance wavelengths for the main reflection maxima are redshifted with respect to the transmission reso-

TABLE I. The wavelengths for maxima and minima in the reflection $R(\lambda)$, transmission $T(\lambda)$, and the flux S_{int}^{d}.

λ(nm) of	R_{max}^{main}	R_{max}^{little}	R_{min}
	276	248	237
	426	377	255, $m=3$
	882	773	356
			389, $m=2$
			714
			802, $m=1$
λ(nm) of	T_{max}	T_{min}	S_{max}^{d}
	260, $m=3$	226	253
	396, $m=2$	315	388
	812, $m=1$	542	802

nances. The wavelengths of both the transmission and reflection (main and little) resonances are redshifted with respect to the Fabry-Perot wavelengths $\lambda_r^m=702$ nm, 351 nm,… ($\lambda_r^m=2b/m, m=1, 2, 3, \ldots$). To understand the physical mechanism of the resonant backward scattering, we also compared the integrated flux $S_{int}^{ird}(U^i,U^r,U^d)$ with the fluxes $S_{int}^{d}(U^d)$ and $S_{int}^{3}(U^3)=T$. As can be seen from Fig. 3(a), the integrated fluxes $S_{int}^{d}(\lambda)$, $S_{int}^{ird}(\lambda)$, and $S_{int}^{3}(\lambda)=T(\lambda)$ are practically undistinguishable also in the λ domain [for the b domain, see Fig. 2(a)]. The difference between the integrated fluxes $S_{int}^{rd}(U^r,U^d)=R$ and $S_{int}^{3}(U^3)=T$ [$T\approx S_{int}^{d}(U^d)$] is caused by the interference of the backward diffracted field $U^d(x,z)$ and the reflected field $U^r(x,z)$ in the energy flux $\vec{S}\sim(\vec{E}\times\vec{H}^*+\vec{E}^*\times\vec{H})$. The wavelengths of the little maxima of the reflection $R=R(U^d,U^r)$ correspond approximately to the high maxima S_{int}^{d}. Therefore the little maxima can be attributed to the interference of the reflected field U^r with the dominant diffracted field U^d. The redshifts and the asymmetrical shapes of the reflection bands can be explained by a Fano analysis[9] of the scattering problem by distinguishing resonant and nonresonant interfering contributions to the reflection process. The resonant contribution is given by the field U^d and the nonresonant one is attributed to the field U^r. Other interesting interpretations of the shifts of resonant wavelengths in the transmission spectra from the values $2b/m$ can be found in Refs. 11, 14–16, 18, and 24. It should be mentioned that the asymmetrical behavior of reflection was observed also in the case of a Fabry-Perot resonator.[25,26] The conditions to achieve such an asymmetry are rested on the existence of dissipative loss in the resonator. There is no explicit loss in the present problem, but the dissipative loss can be substituted by radiative loss due to the diffraction by the slit.

After the analysis of Fig. 2(a), it is not surprising that the maxima of the transmission are accompanied by the minima of the reflection also in the λ domain [see Fig. 3(a)]. It should be noted in this connection that such a behavior of $R(\lambda)$ and $T(\lambda)$ is similar to that observed in the case of excitation of the surface plasmons in an array of slit in a thin metal film.[19] In the study,[19] the minima in reflection spectra corresponding to the maxima in the transmission spectra were attributed to the redistribution of the energy of diffracted evanescent order into the propagating order. In the case of a thick film, we explain such a behavior by another physical mechanism, the interference of the backward diffracted field $U^d(x,z)$ and the reflected field $U^r(x,z)$. It can be noted that the correlation of positions of reflection minima and transmission maxima [see Figs. 2(a) and 3(a)] are consistent with that predicted by Ref. 18 for TE-polarized light scattered by a grating of two-side-open slits in a thick metal film. However, the values of $R(\lambda)$ and $T(\lambda)$ are in contrast to the relation $R(\lambda)+T(\lambda)=1$ given in the study.[18] The difference can be explained by the fact that we examined light scattering by an infinite screen using local definitions of R and T, while Ref. 18 analyzed the global reflection and transmission by a grating of finite size.

The dispersions $S_{int}^{d}(\lambda)$, $S_{int}^{ird}(\lambda)$, and $S_{int}^{3}(\lambda)=T(\lambda)$ shown in Fig. 3(a) indicate the wave-cavity interaction behavior, which is similar to that in the case of a Fabry-Perot resonator. The fluxes $S_{int}^{d}(U^d)$, $S_{int}^{ird}(U^i,U^r,U^d)$, and $S_{int}^{3}(U^3)=T$ exhibit the Fabry-Perot-like maxima around the resonance wavelengths $\lambda_r^m\approx 2b/m$. In order to understand the connection between the Fabry-Perot-like resonances and the total reflection, we computed the amplitude and phase distributions of the light wave at the resonant and near-resonant wavelengths inside and outside the slit cavity [see Figs. 3(b), 4, and 5]. At the resonance wavelengths, the intraslit fields possess maximum amplitudes with Fabry-Perot-like spatial distributions [Fig. 3(b)]. However, in contrast to the Fabry-Perot-like modal distributions, the resonant configurations are characterized by antinodes of the electric field at each open aperture of the slit. Such a behavior is in agreement with the results of Refs. 11, 21, and 22. It is interesting that at the slit entrance, the amplitudes E_x of the resonant field configuration possesses the Fabry-Perot-like phase shift on the value of π (Fig. 4). The integrated fluxes $S_{int}^{ird}(U^i,U^r,U^d)$, $S_{int}^{d}(U^d)$, and $S_{int}^{3}(U^3)$, at the first resonant wavelength λ_r^1, exhibit enhancement by a factor $\lambda/2\pi a\approx 10$ with respect to the incident wave [Fig. 3(a)]. For the comparison, the normalized resonant fluxes $S_n^{ird}(U^i,U^r,U^d)$ and $S_n^{3}(U^3)$ in the near-field zone ($z\approx -2a$) are about five times greater than the incident wave (see Fig. 5). It should be stressed that the resonantly enhanced intracavity intensity $S_n^{2}(U^2)$ is about ten times higher than the resonant fluxes $S_n^{ird}(U^i,U^r,U^d)$ and $S_n^{3}(U^3)$ localized in the near field zone in front of the slit and behind the slit, respectively (Fig. 5). The interference of the incident $U^i(x,z)$ wave and the backward scattered fields $U^r(x,z)$ and $U^d(x,z)$, at the resonant wavelengths $\lambda_r^m\approx 2b/m$, produces in the near-field diffraction zone a strongly localized wave whose normalized flux $S_n^{ird}(U^i,U^r,U^d)$ is $\lambda/2\pi a\approx 10-10^3$ times greater than the incident wave, but about one order of magnitude smaller than the resonant intracavity intensity.

In our model we considered an incident wave with TM polarization. According to the theory of waveguides, the vectorial wave equations for this polarization can be reduced to one scalar equation describing the magnetic field H of TM modes. The electric component E of these modes is found using the field H and Maxwell's equations. The TM scalar equation for the component H is decoupled from the similar

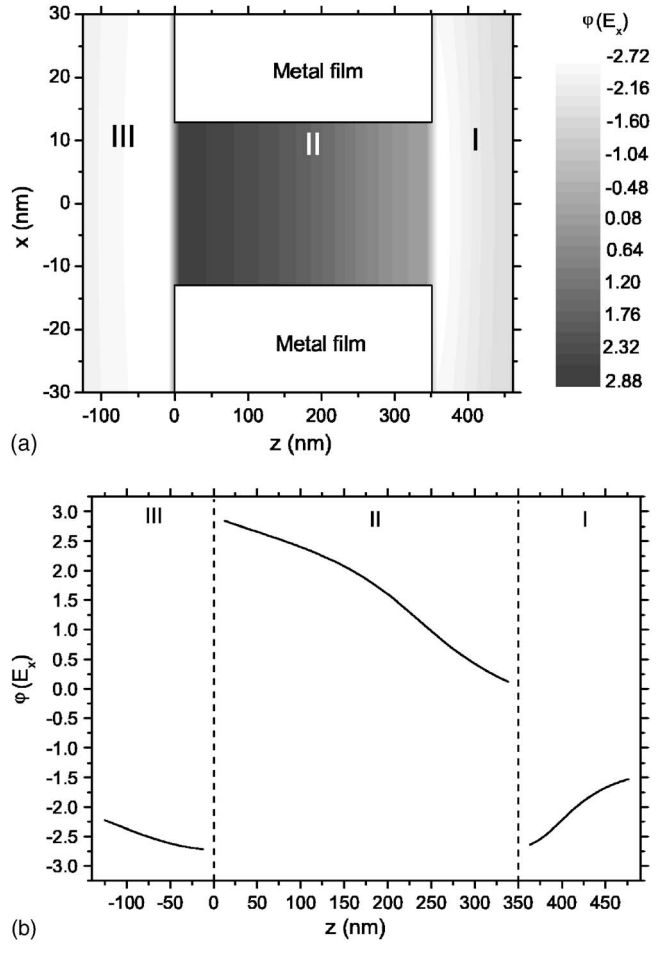

FIG. 4. (a) The phase distribution $\varphi(x,z)$ of the electric-field x component $E_x(x,z)$ inside and outside the slit. The field component $E_x(x,z)$ is given by $E_x(U^i,U^r,U^d)$, $E_x(U^2)$, and $E_x(U^3)$ in regions I, II, and III, respectively. (b) The phase distribution $\varphi(x,z)$ at $x=0$. The slit width $2a=25$ nm, the film thickness $b=351$ nm, and the wavelengths $\lambda=800$ nm.

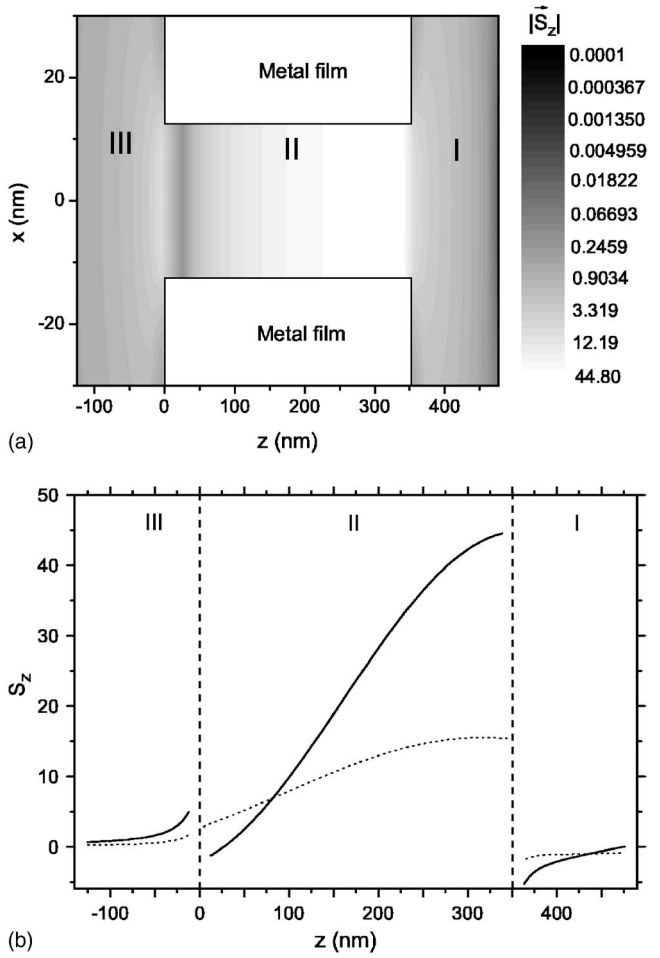

FIG. 5. (a) The spatial distribution $|\vec{S}_z(x,z)|$ of the absolute value of the normalized energy flux along the z direction inside and outside the slit. The distribution $|S_z(x,z)|$ is shown in the logarithmical scale. The flux S_z is given by the normalized fluxes $S^{ird}(U^i,U^r,U^d)/S^i(U^i)$, $S^2(U^2)/S^i(U^i)$, and $S^3(U^3)/S^i(U^i)$ for the regions I, II, and III, respectively. (b) The energy flux distribution $S_z(x,z)$ at $x=0$. The slit width $2a=25$ nm, the film thickness $b=351$ nm, and the wavelengths $\lambda=800$ nm (solid line) and $\lambda=882$ nm (dotted line) corresponding to a transmission resonance and a little reflection resonance, respectively.

scalar equation describing the field E of TE (transverse electric) modes. Hence the formalism works analogously for TE polarization exchanging the E and H fields.

III. SUMMARY AND CONCLUSION

In the present paper, the backward scattering of TM-polarized light by a two-side-open subwavelength slit in a metal film has been analyzed. We predict that the reflection coefficient versus wavelength possesses a Fabry-Perot-like dependence that is similar to the anomalous behavior of transmission. The open slit totally reflects the light at the near-to-resonance wavelengths. The resonance wavelengths for the total reflection are somewhat redshifted with respect to the transmission resonances. The wavelengths of both the reflection and transmission resonances are redshifted with respect to the Fabry-Perot wavelengths. The sharp resonant maxima of transmission are accompanied by the wide minima of the reflection. In addition, we showed that the interference of incident and resonantly backward-scattered light produces in the near-field diffraction zone a strongly localized wave whose intensity is greater than the incident wave by a factor $\lambda/2\pi a \approx 10-10^3$ and about one order of magnitude smaller than the intracavity intensity. The correlation between the amplitude and phase distributions of light waves inside and outside the slit was also investigated. The slit cavity was compared with a Fabry-Perot resonator. We showed that the amplitude and phase of the resonant wave at the slit entrance and exit are different from that of a Fabry-Perot cavity. The physical mechanism responsible for the total reflection is the interference of the backward diffracted resonant field $U^d(x,z)$ and the reflected nonresonant field $U^r(x,z)$ in the energy flux at the near-to-resonance wavelengths (Fano-type effect). The wavelength-selective total reflection of light by two-side-open metal slits may find application in many kinds of sensors and actuators. The $(10-10^3)$-times and (10^2-10^4)-times enhancement of the

light intensity in front of the slit and inside the slit can be used in reflective nano-optics and in intracavity spectroscopy of single atoms. We believe that the presented results gain insight into the physics of resonant scattering of light by subwavelength nanoslits in metal films.

ACKNOWLEDGMENTS

This study was supported by the Fifth Framework of the European Commission (financial support from the EC for shared-cost RTD actions: research and technological development projects, demonstration projects, and combined projects, Contract No. NG6RD-CT-2001-00602) and in part by the Hungarian Scientific Research Foundation (OTKA, Contract Nos. T046811 and M045644), and the Hungarian R&D Office (KPI, Contract No. GVOP-3.2.1.-2004-04-0166/3.0).

APPENDIX

We briefly describe the Neerhoff and Mur model[1,3] of the scattering of a continuous plane wave by a subwavelength slit of width $2a$ in a perfectly conducting metal screen of thickness b. The slit is illuminated by a normally incident plane wave under TM polarization (magnetic-field vector parallel to the slit), as shown in Fig. 1. The magnetic field of the wave is assumed to be time harmonic and constant in the y direction:

$$\vec{H}(x,y,z,t) = U(x,z)e^{-i\omega t}\vec{e}_y. \tag{A1}$$

The electric field of the wave is found from the scalar field $U(x,z)$ using Maxwell's equations. The restrictions in Eq. (1) reduce the diffraction problem to one involving a single scalar field $U(x,z)$ in two dimensions. The field is represented by $U_j(x,z)$ ($j=1$, 2, 3 in regions I, II, and III, respectively), and satisfies the Helmholtz equation: $(\nabla^2+k_j^2)U_j=0$, where $j=1$, 2, 3. In region I, the field $U_1(x,z)$ is decomposed into three components:

$$U_1(x,z) = U^i(x,z) + U^r(x,z) + U^d(x,z), \tag{A2}$$

each of which satisfies the Helmholtz equation. U^i represents the incident field:

$$U^i(x,z) = e^{-ik_1 z}. \tag{A3}$$

U^r denotes the reflected field without a slit:

$$U^r(x,z) = U^i(x,2b-z). \tag{A4}$$

Finally, U^d describes the diffracted field in region I due to the presence of the slit. With the above set of equations and standard boundary conditions for a perfectly conducting screen, a unique solution exists for the scattering problem. The solution is found by using the Green-function formalism.

The magnetic $\vec{H}(x,z,t)$ fields in regions I, II, and III are given by

$$H^1(x,z) = \exp(-ik_1 z) + \exp[-ik_1(2b-z)] - \frac{ia}{N}\frac{\epsilon_1}{\epsilon_2}\sum_{j=1}^{N} H_0^1[k_1\sqrt{(x-x_j)^2+(z-b)^2}](DU_b)_j, \tag{A5}$$

$$\begin{aligned} H^2(x,z) = &-\frac{i}{2N\sqrt{k_2^2}}e^{i\sqrt{k_2^2}|z|}\sum_{j=1}^{N}(DU_0)_j + \frac{i}{2N\sqrt{k_2^2}} \\ &\times e^{i\sqrt{k_2^2}|z-b|}\sum_{j=1}^{N}(DU_b)_j - \frac{1}{2N}e^{i\sqrt{k_2^2}|z|}\sum_{j=1}^{N}(U_0)_j + \frac{1}{2N} \\ &\times e^{i\sqrt{k_2^2}|z-b|}\sum_{j=1}^{N}(U_b)_j - \frac{i}{N}\sum_{m=1}^{\infty}\frac{1}{\gamma_1}\cos\frac{m\pi(x+a)}{2a}e^{i\gamma_1|z|} \\ &\times \sum_{j=1}^{N}\cos\frac{m\pi(x_j+a)}{2a}(DU_0)_j - \frac{1}{N}\sum_{m=1}^{\infty}\cos\frac{m\pi(x+a)}{2a} \\ &\times e^{i\gamma_1|z|}\sum_{j=1}^{N}\cos\frac{m\pi(x_j+a)}{2a}(U_0)_j + \frac{i}{N}\sum_{m=1}^{\infty}\frac{1}{\gamma_1}e^{i\gamma_1|z-b|} \\ &\times \cos\frac{m\pi(x+a)}{2a}\sum_{j=1}^{N}\cos\frac{m\pi(x_j+a)}{2a}(DU_b)_j \\ &+ \frac{1}{N}\sum_{m=1}^{\infty}\cos\left(m\pi\frac{x+a}{2a}\right)e^{i\gamma_1|z-b|} \\ &\times \sum_{j=1}^{N}\cos\frac{m\pi(x_j+a)}{2a}(U_b)_j, \end{aligned} \tag{A6}$$

$$H^3(x,z) = i\epsilon_3\sum_{j=1}^{N}\frac{a}{N\epsilon_2}(D\vec{U}_0)_j H_0^{(1)}[k_3\sqrt{(x-x_j)^2+z^2}], \tag{A7}$$

where $x_j=2a(j-1/2)/N-a$, $j=1,2,\ldots,N$; $N>2a/z$; $H_0^{(1)}(X)$ is the Hankel function; $\vec{H}^i=H^i\cdot\vec{e}_y$, $i=1$, 2, 3; $\gamma_m=[k_2^2-(m\pi/2a)^2]^{1/2}$. The coefficients $(D\vec{U}_0)_j$ are found by solving numerically four coupled integral equations. For more details on the model and the numerical solution of the Neerhoff and Mur coupled integral equations, see Refs. 1 and 3.

[1] F. L. Neerhoff and G. Mur, Appl. Sci. Res. **28**, 73 (1973).

[2] R. F. Harrington and D. T. Auckland, IEEE Trans. Antennas Propag. **AP28**, 616 (1980).

[3] E. Betzig, A. Harootunian, A. Lewis, and M. Isaacson, Appl. Opt. **25**, 1890 (1986).

[4] T. W. Ebbesen, H. J. Lezec, H. F. Ghaemi, T. Thio, and P. A. Wolff, Nature (London) **391**, 667 (1998).

[5] A. Hessel and A. A. Oliner, Appl. Opt. **4**, 1275 (1965).

[6] M. Nevière, D. Maystre, and P. Vincent, J. Opt. **8**, 231 (1977).
[7] D. Maystre and M. Nevière, J. Opt. **8**, 165 (1977).
[8] V. U. Fano, Ann. Phys. **32**, 393 (1938).
[9] M. Sarrazin, J. P. Vigneron, and J. M. Vigoureux, Phys. Rev. B **67**, 085415 (2003).
[10] J. A. Porto, F. J. García-Vidal, and J. B. Pendry, Phys. Rev. Lett. **83**, 2845 (1999).
[11] S. Astilean, Ph. Lalanne, and M. Palamaru, Opt. Commun. **175**, 265 (2000).
[12] A. P. Hibbins, J. R. Sambles, and C. R. Lawrence, Appl. Phys. Lett. **81**, 4661 (2002).
[13] Q. Cao and P. Lalanne, Phys. Rev. Lett. **88**, 057403 (2002).
[14] Y. Takakura, Phys. Rev. Lett. **86**, 5601 (2001).
[15] F. Yang and J. R. Sambles, Phys. Rev. Lett. **89**, 063901 (2002).
[16] S. V. Kukhlevsky, M. Mechler, L. Csapo, K. Janssens, and O. Samek, Phys. Rev. B **70**, 195428 (2004).
[17] F. J. García-Vidal, H. J. Lezec, T. W. Ebbesen, and L. Martín-Moreno, Phys. Rev. Lett. **90**, 213901 (2003).
[18] A. G. Borisov, F. J. Garcia de Abajo, and S. V. Shabanov, Phys. Rev. B **71**, 075408 (2005).
[19] J. M. Steele, C. E. Moran, A. Lee, C. M. Aguirre, and N. J. Halas, Phys. Rev. B **68**, 205103 (2003).
[20] F. J. García-Vidal and L. Martín-Moreno, Phys. Rev. B **66**, 155412 (2002).
[21] J. Lindberg, K. Lindfors, T. Setala, M. Kaivola, and A. T. Friberg, Opt. Express **12**, 623 (2004).
[22] Y. Xie, A. R. Zakharian, J. V. Moloney, and M. Mansuripur, Opt. Express **12**, 6106 (2004).
[23] U. Schröter and D. Heitmann, Phys. Rev. B **58**, 15419 (1998).
[24] M. M. J. Treacy, Appl. Phys. Lett. **75**, 606 (1999).
[25] J. J. Monzón and L. L. Sánchez-Soto, J. Opt. Soc. Am. A **12**, 132 (1995).
[26] R. Giust, J. M. Vigoureux, and M. Sarrazin, J. Opt. Soc. Am. A **17**, 142 (2000).
[27] E. Popov, M. Nevière, S. Enoch, and R. Reinisch, Phys. Rev. B **62**, 16100 (2000).
[28] S. I. Bozhevolnyi, J. Erland, K. Leosson, P. M. W. Skovgaard, and J. M. Hvam, Phys. Rev. Lett. **86**, 3008 (2001).
[29] A. Barbara, P. Quemerais, E. Bustarret, and T. Lopez-Rios, Phys. Rev. B **66**, 161403(R) (2002).
[30] A. M. Dykhne, A. K. Sarychev, and V. M. Shalaev, Phys. Rev. B **67**, 195402 (2003).
[31] X. L. Shi, L. Hesselink, and R. L. Thornton, Opt. Lett. **28**, 1320 (2003).
[32] H. F. Schouten, T. D. Visser, D. Lenstra, and H. Blok, Phys. Rev. E **67**, 036608 (2003).
[33] A. Nahata, R. A. Linke, T. Ishi, and K. Ohashi, Opt. Lett. **28**, 423 (2003).
[34] A. Bouhelier, M. Beversluis, A. Hartschuh, and L. Novotny, Phys. Rev. Lett. **90**, 013903 (2003).
[35] K. Li, M. I. Stockman, and D. J. Bergman, Phys. Rev. Lett. **91**, 227402 (2003).
[36] A. Dechant and A. Y. Elezzabi, Appl. Phys. Lett. **84**, 4678 (2004).
[37] W. J. Fan, S. Zhang, B. Minhas, K. J. Malloy, and S. R. J. Brueck, Phys. Rev. Lett. **94**, 033902 (2005).
[38] A. V. Zayats, I. I. Smolyaninov, and A. A. Maradudin, Phys. Rep. **408**, 131 (2005).
[39] M. Labardi, M. Zavelani-Rossi, D. Polli, G. Cerullo, M. Allegrini, S. De Silvestri, and O. Svelto, Appl. Phys. Lett. **86**, 031105 (2005).
[40] Y. Ben-Aryeh, Int. J. Quantum Inf. **3**, 111 (2005).